



Reliability study under thermal and photonic stresses of sulforhodamine B (SRB) confined in layered double hydroxide (LDH)

Paul Legentil, Fabrice Leroux, Sandrine Therias, Damien Boyer, François
Réveret, Geneviève Chadeyron

► To cite this version:

Paul Legentil, Fabrice Leroux, Sandrine Therias, Damien Boyer, François Réveret, et al.. Reliability study under thermal and photonic stresses of sulforhodamine B (SRB) confined in layered double hydroxide (LDH). Applied Clay Science, 2020, pp.105922. 10.1016/j.clay.2020.105922 . hal-03016985

HAL Id: hal-03016985

<https://uca.hal.science/hal-03016985>

Submitted on 20 Nov 2020

HAL is a multi-disciplinary open access archive for the deposit and dissemination of scientific research documents, whether they are published or not. The documents may come from teaching and research institutions in France or abroad, or from public or private research centers.

L'archive ouverte pluridisciplinaire **HAL**, est destinée au dépôt et à la diffusion de documents scientifiques de niveau recherche, publiés ou non, émanant des établissements d'enseignement et de recherche français ou étrangers, des laboratoires publics ou privés.



Distributed under a Creative Commons Attribution 4.0 International License

Reliability study under thermal and photonic stresses of sulforhodamine B (SRB) confined in layered double hydroxide (LDH).

Paul Legentil¹, Fabrice. Leroux^{1*}, Sandrine Therias¹, Damien Boyer¹, François Reveret², Geneviève Chadeyron^{1*}

¹ Université Clermont Auvergne, CNRS, SIGMA Clermont, ICCF, F-63000 Clermont–Ferrand, France.

² Université Clermont Auvergne, CNRS, SIGMA Clermont, Institut Pascal, F-63000 Clermont–Ferrand, France.

*e-mail genevieve.chadeyron@sigma-clermont.fr, fabrice.leroux@uca.fr

ABSTRACT

When sulforhodamine B (SRB) is entrapped in a tightly packed hybrid material composed of dodecylsulfate anions interleaved in layered double hydroxide, the organic dye is considered as a possible red-emitting phosphor for white light-emitting diodes (WLEDs). To confirm such promising potential, a reliability study is here undertaken and the materials and their associated silicone films are subjected to different thermal and photonic stresses. Optical properties, photoluminescence quantum yields and emission spectra are recorded after photo-aging studies. Interestingly, the composite silicone film is found to be completely stable under blue LED excitation, while in the absence of the hybrid LDH the emission of SRB decays rapidly, thus underlining the protective role of the LDH hybrid cargo. At this stage, these results confirm the potential offered by a system consisting of such an emitter film and a blue LED. This system also opens up new possibilities for interesting organic dyes that are sensitive to photonic and/or thermal stresses.

1. Introduction

In lighting applications, white light-emitting diodes (WLED) are now emerging very strongly and constitute a reference in solid-state lighting sources because of their excellent properties, such as high light efficiency, energy-saving properties, long lifetime and absence of toxic mercury or other heavy metals. A commercial WLED consists of a blue chip, emitting between 450 and 480 nm, combined with a yellow-emitting phosphor (Nair et al., 2020), YAG:Ce³⁺ (yttrium aluminium garnet doped with Ce³⁺ cations), and a red-emitting phosphor is commonly added to improve the colorimetric characteristics of light (Xia et al., 2016). A recent study concerning a well-known organic dye, sulforhodamine B (SRB), underlined its interest as a red phosphor and its potential under commercial blue LED excitation when highly dispersed in a host structure, layered double hydroxide (LDH) (Legentil et al., 2020). Indeed, the inorganic LDH vessel intercalated with surfactant molecules (dodecylsulfate (DS)) is found to display a suitable arrangement for SRB to be well ensconced, avoiding intermolecular interactions deleterious for the red emission as well as providing an affinity with silicone in the preparation of homogeneous films. The properties of an optimized system composed of alternating a blue chip, a YAG: Ce³⁺/silicone composite film and a LDH-DS-SRB/silicone composite film are satisfactorily met, with a correlated color temperature (T(K)) associated with a color rendering index (CRI) suitable for a commercial WLED application.

LEDs are known to have an operating temperature of up to 100 or 120°C, and hence phosphors must have the ability to sustain such harsh conditions without any degradation

Several studies have been undertaken on inorganic phosphors. Da Lago et al.(Dal Lago et al., 2012) published one of the first reliability studies concerning a commercial YAG: Ce phosphor under thermal stresses (between 85 and 145 °C) for remote-phosphor technology. Thus, it was demonstrated that the heat generated can significantly limit the lifetime as well as the performance of the phosphor. We can also mention the works of Shao et al (Shao et al., 2014), which have shown the modification of the color coordinates and the spectral shift of BaSiO₄: Eu²⁺ emission (a green-emitting phosphor under blue LED excitation) with respect to temperature. In order to provide better thermal stability, they suggested substituting the Ba sites by Sr atoms in this phosphor, and in this way they succeeded in lowering thermal quenching. Since then, other works have reported the limited stability of phosphors formulated with rare earth elements under thermal stresses (Yazdan Mehr et al., 2014; Zhou et al., 2014).

However, the reliability of organic phosphors has scarcely been reported so far. Indeed, the use of organic dyes for WLED applications is appealing in terms of their luminescence properties but the stability studies are only superficial (Boonsin et al., 2015; Kajjam et al., 2018). As mentioned before, to further address a practical application in commercial lighting devices, a major specification required of the fluorophore and its associated system is to present long-term stability with respect to various types of stress in real operating conditions. Several published works mentioned the use of fluorophore with a potential application for replacing traditional phosphors with rare earth elements in commercial WLED, such as fluorescein, pyranine, rhodamine or triphenylamine derivatives for instance (Das and Manam, 2018; Legentil et al., 2019; Nyalosaso et al., 2019; Zhang et al., 2008). However, the authors do not usually pay attention to the reliability of the dyes in stressful conditions.

Traditionally, LDH materials find applications as precursors in catalysis and as scavengers in environmental science, but are also finding renewed interest in the domain of energy (Wu et al., 2018; Yin et al., 2019) as well as in biology as vessels for drug delivery (Conterposito et al., 2016; Lonkar et al., 2013; Yan et al., 2014). Their general chemical formula is as follows

$[M(II)_{1-x}M(III)_x(OH)_2]^{x+}[A^{n-}]_{x/n} \cdot mH_2O$ where M(II) is a divalent cation such as Zn^{2+} , Mg^{2+} , Fe^{2+} , etc... and M(III) a trivalent cation such as Al^{3+} , Fe^{3+} , etc. and A^{n-} is an interleaved anion. The anisotropic two-dimensional structure is built from edge-sharing octahedral. Compared to brucite $Mg(OH)_2$, the partial substitution of divalent cations by trivalent cations implies for LDH sheets a net positive charge. To ensure electroneutrality, anions of interest, here the dye molecules together with the surfactant molecules, are located in the interlayer space of the LDH with the presence of water molecules.

Importantly, organic dyes are known to be sensitive to different stresses (thermal, photonic...) (Lamouche et al., 1999; Sultana, 2018). To overcome such issues, an elegant solution consists in immobilizing the SRB molecules in an inorganic host lattice like layered double hydroxide (LDH) as previously reported (Legentil et al., 2020). Pioneer research has underlined the benefit of confining photoactive species to a restricted space such as a two-dimensional host in terms of 1) their strong adsorption through host-guest interaction to avoid possible migration and aggregation within a polymer, and 2) their dispersion with the presence of co-adsorbates to avoid as far as possible guest-guest interactions (Ogawa and Kuroda, 1995). However, a reliability study of such a hybrid organic dye/LDH host matrix for LED applications must be conducted before considering any practical application; this aspect has never been published to the best of our knowledge.

In the following, a reliability study of the SRB dye in the presence of thermal and photonic stresses in different conditions when placed in a LED set-up is presented in order to confirm the promising features of the synthesized hybrid LDH-SRB. To address this issue, comparative studies were performed, first on the hybrid LDH/SRB powder and then on a composite film by dispersing the powder in silicone polymer. In the first case only temperature effects were studied. Then, both thermal and photonic stresses were concomitantly applied and recorded for silicone films. Behaviour in accelerated photo-aging was also observed. Photoluminescence properties such as emission spectra and photoluminescence quantum yields were scrutinized during all the different tests to better understand the mechanisms involved in the loss of optical properties.

2. Experimental section

2.1. Materials

Sulforhodamine B sodium salt $C_{27}H_{30}N_2NaO_7S_2$, sodium dodecylsulfate $CH_3(CH_2)_{11}OSO_3Na$ and terephthalic acid $C_8H_6O_4$ were purchased from Sigma-Aldrich, and YAG:Ce³⁺ from Phosphortech. $Zn(NO_3)_2 \cdot 6H_2O$ (purity 99.9+%), $Al(NO_3)_3 \cdot 9H_2O$ (purity 99.9+%) and NaOH (97%) were obtained from Sigma Aldrich. The two-component silicone elastomer, Bluesil RTV 141 part A and part B, was supplied by Elkem.

2.2. Synthesis procedure for LDH hybrid materials using the coprecipitation method

The sulforhodamine B (SRB)-dodecylsulfate (DS) LDH phase, Zn_2Al -DS-SRB, called LDH-DS-SRB, was prepared using the coprecipitation method. The synthesis of $[Zn_2Al_1(OH)_6]^+[DS^-]_{1-x}[SRB^-]_x \cdot mH_2O$ was performed using 50 mL of sulforhodamine B and dodecylsulfate aqueous solution (with de-ionized water). 50 mL of an aqueous solution of Zn^{2+} (3.2 mmol) and Al^{3+} (1.6 mmol) was added dropwise over a period of 3 hours under magnetic stirring. To synthesize the $[Zn_2Al_1(OH)_6]^+[DS^-]_{0.9995}[SRB^-]_{0.0005} \cdot mH_2O$ sample, 0.8×10^{-3} mmol and 1.5992 mmol were used for SRB salt and sodium dodecylsulfate, respectively. This formulation was determined in a previous article as that leading to the best optical performance under commercial blue LED and UV excitation (Legentil et al., 2020).

The pH was maintained at 8.5 by adding 0.25 M NaOH during the synthesis process. Coprecipitation was performed under nitrogen at 20 °C. The mixture was centrifuged at 5,000 rpm for 5 minutes and the slurry on the bottom of the flask was then washed several times with de-ionized water until a clear and transparent supernatant was obtained. A paste was recovered and dried overnight at room temperature to obtain the LDH-DS-SRB powder.

The post-synthesis hydrothermal treatment was performed by dispersing the paste, obtained before the drying step, in 20 ml of de-ionized water in a sealed container at 110 °C under autogenous pressure during 48 hours. The slurry was then centrifuged (5 minutes at 5,000 rpm) and the paste was dried overnight at room temperature to obtain the LDH-DS-SRB-TH powder.

Similarly, the terephthalate LDH phase, Zn₂Al-TP-SRB, was prepared by following the method previously described for LDH-DS-SRB by replacing DS by terephthalic acid (TP). However, TP being dianionic, the input of TP was half the molar concentration compared to DS.

2.3. Elaboration of Silicone/HDL-DS-SRB composite films

The LDH-DS-SRB powder was used to produce the silicone/hybrid composite material. A loading rate of 40 wt. % was chosen (beyond this loading rate, it was difficult to obtain a homogeneous distribution of the powder in the polymer matrix, as shown in figure S1). The two-component silicone elastomer (silicone Bluesil-RTV 141 A&B) was composed of a viscous liquid, called part A, cured by a polyaddition reaction with a catalyser, part B.

The silicone/hybrid composite material was manufactured by mixing the LDH powder with part A of the silicone elastomer using a mechanical mixer ("Thinky Mixer") for 10 min at 1200 rpm. Then the obtained mixture was processed through a three-roll Exakt80E (spacing of 30 µm between the first two rolls and 50 µm between the last two rolls) to achieve a better dispersion of the LDH platelets by shearing and to obtain a homogeneous hybrid component. Part B was added at 10phr and further homogenised using the mechanical mixer for 10 min at 1200 rpm.

The silicone/hybrid composite film (Si-LDH) was prepared by casting onto a Teflon surface using an Elcometer 4340 automatic film applicator. The knife blade height was set at 200 µm and the casting speed was 30 mm/s. This two-component silicone film was cured at 80 °C for 2 hours.

A reference film composed of SRB powder dispersed in the silicone, called Si-SRB, was also performed by dispersing 100 µL of an SRB solution in ethylene glycol (10 g.L⁻¹) in 4.45 g of part A of the silicone elastomer using the "Thinky Mixer" mechanical mixer for 10 min at 1200 rpm. Then 0.45 g of part B was added and homogenised with the mechanical mixer for 10 min at 1200 rpm. The film was prepared by casting onto a Teflon surface in the same way as for Si-LDH mentioned above.

Film thickness was measured using an Elcometer 456 coating thickness gauge.

2.4. Characterisation

2.4.1. X-ray diffraction

LDH powders were characterised by X-Ray Diffraction; the XRD patterns were recorded with a Philips X-Pert Pro diffractometer operating with Cu-Kα radiation ($\lambda = 1.5418 \text{ \AA}$). The data were collected in a 2θ range between 5° and 70° with a step size of 1°/min.

2.4.2. Thermogravimetric analysis

Thermogravimetric (TG) analyses were performed on a Setaram TGA 92 instrument with a linear heating rate of 5 °C.min⁻¹ under air.

2.4.3. UV-Visible absorption

The UV–visible absorption spectra of the samples were recorded in a wavelength range of 200 to 800 nm with a UV–vis spectrophotometer (SP-3000 Plus) equipped with an integrating sphere and UV-Probe software.

2.4.4. Luminescence

Quantum yield efficiencies and emission spectra were measured using a C9920-02G PL-QY integrating sphere measurement system from Hamamatsu Photonics. The setup consisted of a 150 W monochromatized Xe lamp, an integrating sphere (Spectralon coating, \varnothing = 3.3 in.) and a high-sensitivity CCD camera.

2.4.5. Emission stability of films under LED irradiation

A photo-aging study was performed in a SEPAP 12/24 unit. This system was designed to achieve accelerated artificial weathering conditions related to natural ageing. The composite films were placed on a rotating carousel positioned in the centre, and four polychromatic mercury lamps (400 W) with wavelengths higher than 300 nm (90 W.m⁻²) were installed at the corners of the chamber. The temperature was set at 60 °C.

Reliability studies were carried out using a home-made setup consisting of a power-controlled blue LED emitting at 460 nm as the excitation source and a HR4000 high resolution spectrometer (Ocean Optics) as the PL analyser. The samples were positioned on a heating element whose temperature was adjusted to 80°C. The emission spectra of the composite films were acquired every 20 min for 24 hours. Their area was integrated to obtain the total emission intensity. LED power was measured using a Scientech Model Mentor MA 10 with a MC2501 calorimetric head unit (25.4 mm aperture). The measurement was performed by centring the head unit over the LED source and measuring the power of the LED light emitted through the aperture. The blue LED power was 183 mW. The LED power density can be expressed in W/m² and was calculated by LED power (in watt) per unit surface of the sample (0.25 cm²). The power density of the blue LED was 9300 W/m²; for our experiments, a filter was used in order to reduce this value to 2480 W/m².

3. Results and discussion

3.1. Hydrothermal post-treatment

3.1.1. Structural effect

X-ray diffractogram patterns of both LDH-DS-SRB and LDH-DS-SRB-HT powders before and after hydrothermal treatment respectively are plotted in Fig. 1. The two patterns closely overlap, and the associated diffraction peaks are located at similar angles in 2 θ . The observed interlamellar space is 2.58 nm for both powders. However, thinner diffraction peaks are observed for LDH-DS-SRB-HT than for LDH-DS-SRB powder, in particular the peaks with h Miller peak indices, underlining the fact that the hydrothermal treatment induced more ordered platelet stacking.

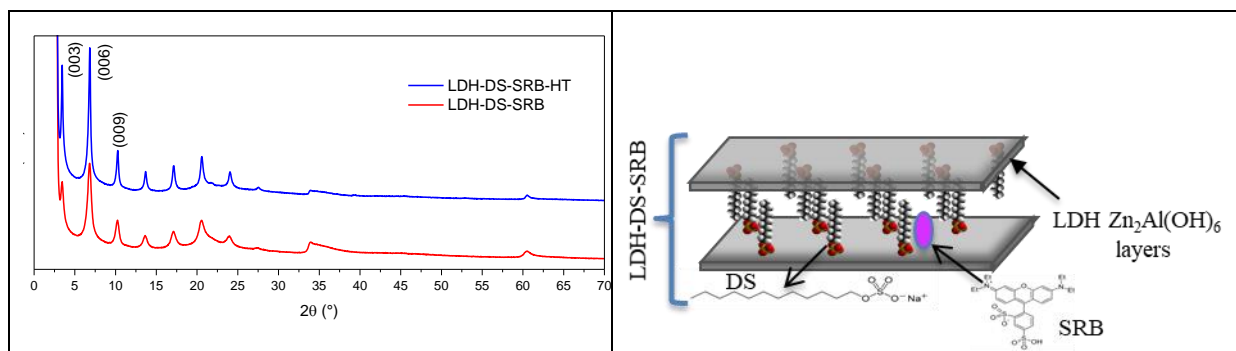


Figure 1. X-ray patterns of LDH-DS-SRB and LDH-DS-SRB-HT powders and on the right an idealized scheme of the LDH-DS-SRB.

The average size of crystallites can be calculated using the Scherrer equation $L = k\lambda/(B \cdot \cos\theta)$ where B is the FWHM (Full Width at Half Maximum) of diffraction peak (003), λ is the Cu K_{α} radiation wavelength in nm, θ is the diffraction angle of (003) in radian et k is the shape factor ($k = 0,9$) (Cullity, 1978). The sizes calculated for LDH-DS-SRB and LDH-DS-SRB-HT are 27.2 nm and 42.3 nm respectively, these values corresponding roughly to 11 and 16 structurally coherent stacked layers, thus confirming a better crystallisation in the stacking direction for LDH-DS-SRB-HT.

As shown in a previous paper (Legentil et al., 2020) and illustrated on the scheme of the Fig.1(right), the sulfonate groups are in the vicinity of the hydroxyl-covered LDH layers, thus leaving the benzene and xanthene rings close to the surfactant alkyl chains. The relative amount of SRB per DS is very small, SRB is highly diluted in the LDH-DS environment.

3.1.2. Optical properties

Internal photoluminescence quantum yields (PL QY_{int}) were recorded from the samples before and after hydrothermal treatment to know whether a change in the ordered stacking may affect the optical response of the interleaved dye molecules (Table 1). Rather counter-intuitively, LDH-DS-SRB-HT powder exhibits lower PL QY_{int} than LDH-DS-SRB. Even if the hydrothermal treatment leaves intact the confinement of the SRB molecules inside the host structure (similar basal spacing is observed), a significant decrease in the luminescence properties is observed for the three excitation wavelengths of interest (570 nm is the excitation wavelength leading to the best PL QY_{ab} and int , (Legentil et al., 2020) (365 nm and 480 nm wavelengths correspond to UV and commercial blue LED, respectively).

Table 1. PL QY_{int} of LDH-DS-SRB and LDH-DS-SRB-HT powder for three excitation wavelengths (570 nm, 480 nm and 365 nm). Three wavelengths are of interest: the 365 nm and 480 nm wavelengths correspond to UV and commercial blue LED respectively, while 570 nm is the excitation wavelength leading to the best PL QY_{ab} .

	Excitation wavelength	LDH-DS-SRB	LDH-DS-SRB-HT
PL QY_{int} (%)	570 nm	73.1 ± 3.5	52.6 ± 2.5
	480 nm	68.9 ± 3.5	42.8 ± 2.1
	365 nm	73.1 ± 3.7	39.0 ± 2.0

We can note that the PL QY_{ab} recorded for these samples before and after hydrothermal treatment (which corresponds to the ratio between the number of photons emitted by the phosphor and the number of photons emitted by the excitation source) leads to the same conclusion (Table S2).

To better understand the modification undergone by the dye molecule, the emission spectra under blue excitation (480 nm) were recorded for both LDH-DS-SRB and LDH-DS-SRB-HT powders (Fig. 2). The emission spectra being similar for the other two excitation wavelengths, they are not presented here. The maximum intensity of the emission band is shifted towards higher wavelengths (from 608 to 614 nm) after the hydrothermal treatment, thus indicating a modification of the environment for the SRB molecules. In detail, the intensity ratio between the main emission peak and the associated shoulder is also modified, with the values of $I_{\text{shoulder1}}/I_{\text{peak1}} = 0.58$ and $I_{\text{shoulder2}}/I_{\text{peak2}} = 0.67$ before and after the hydrothermal treatment, respectively. Since the main peak is attributed to SRB monomer molecules and the shoulder peak to SRB aggregates (dimer and trimer) (Ray and Nakahara, 2002; Yan et al., 2009), the hydrothermal treatment leads to a greater aggregation of the SRB molecules into the LDH-DS hybrid material.

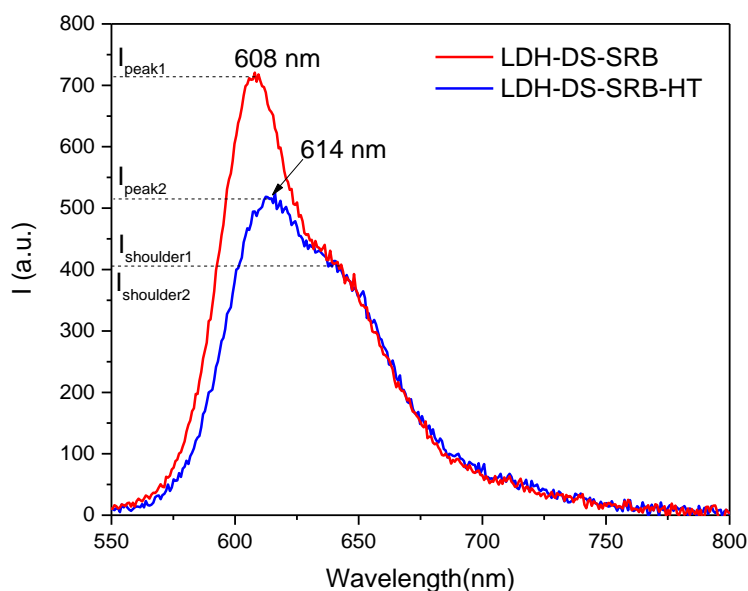


Figure 2. Emission spectra of LDH-DS-SRB and LDH-DS-SRB-HT for $\lambda_{\text{exc}} = 480$ nm

From these observations, the LDH-DS-SRB sample without hydrothermal treatment is selected in the following.

3.2. Effect of thermal stress

3.2.1. Powder LDS-DS-SRB

Thermogravimetric analyses (TGA)

Thermogravimetric analysis shows that the SRB molecule is stable up to about 220 °C (Fig. 3a). Below 100 °C, the mass loss can be attributed to the departure of the weakly-adsorbed water

molecules (weight loss n°1 of 6,8% around 80-100 °C). After 220 °C, decomposition of the SRB molecules (weight loss n°2, 3 and 4) occurs until the final mass loss observed at 500 °C.

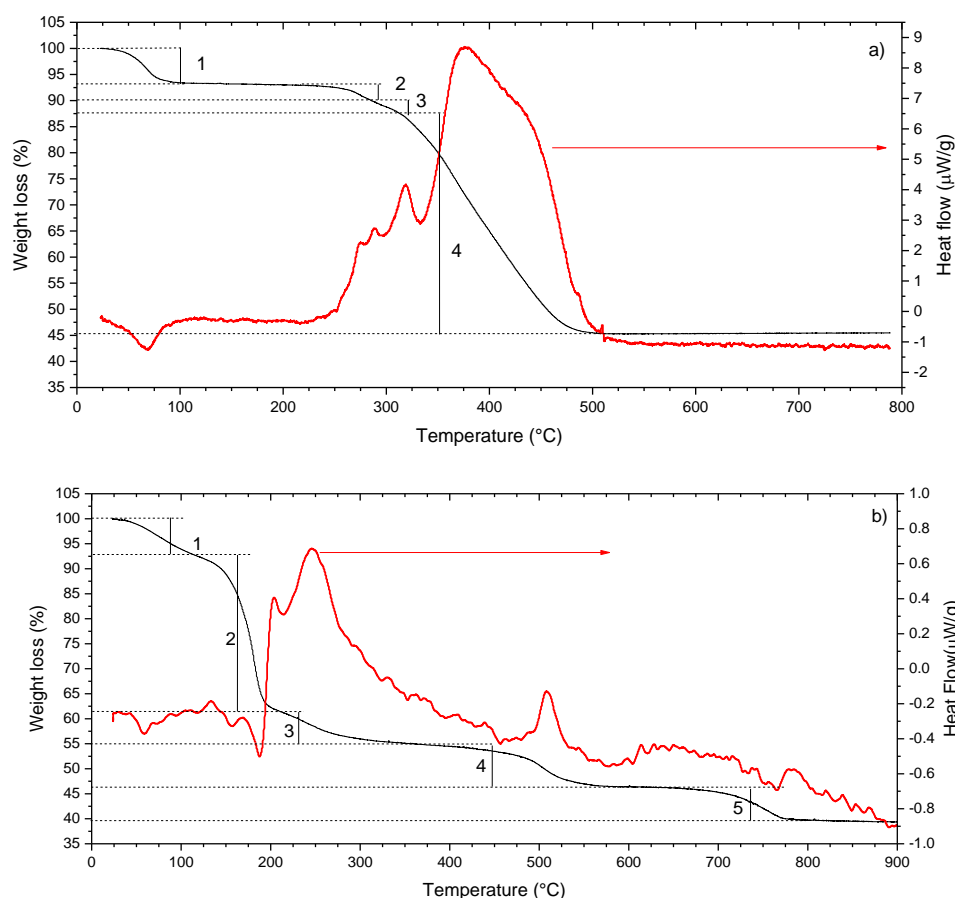


Figure 3. Thermogravimetric analysis and heat flow of a) SRB (2 °C/min, 25 °C- 800 °C, under air) and b) LDH-DS-SRB powder (2 °C/min, 25 °C-1000 °C, under air).

For the hybrid LDH-DS-SRB material, several mass losses are observed. After the water molecules that are weakly bound to the surface of the HDL platelets have been removed (weight loss 1), deshydroxylation of the LDH layers occurs from 180 up to 300 °C, concomitantly with the decomposition of the interleaved organic molecules (weight losses 2 and 3). This is consistent with DS decomposition, well documented in the literature (Degoutin et al., 2008; El-kharrag et al., 2011). The associated mass loss starts at 200 °C and continues up to 400 °C. The mass loss observed at 500 °C is attributed to the final decomposition of the organic residue, while the mass loss at around 740 °C is assigned to the decomposition of ZnSO_4 formed during the thermal treatment with the collapse of the LDH layers reacting with the functionalized head of the surfactant (as well as possibly SRB).

Thermal stress in oven (120 °C)

The thermal stability study was completed in static conditions by placing the LDH-DS-SRB in an oven at 120 °C for 24 hours. X-ray diffraction patterns were recorded after 5 and 24 hours (Fig. 4).

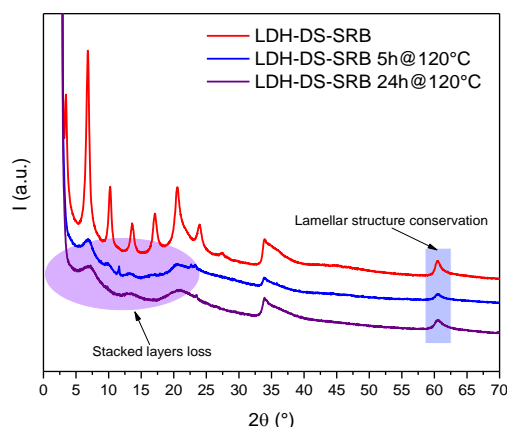


Figure 4. X-ray diffraction patterns of LDH-DS-SRB powder before after thermal treatment (5 and 24 hours)

After both exposure times at 120 °C, the LDH-DS-SRB powder exhibits a similar XRD pattern. As the peak at 61 ° in 2θ assigned to the diffraction peak (110) merged with (113) is still observed, this is indicative that the LDH layer structure is maintained. However, the harmonic peaks (00 l), visible at angles lower than 25 ° (2θ) attributed to the strongly pronounced stacking for LDH-DS-SRB disappear after the thermal treatment at 120 °C. Only a few peaks of relatively low intensity are observed; the first peak located at $2\theta = 7.5^{\circ}$ corresponds to a basal spacing of 11.8 nm. Unexpectedly at this low temperature, this strong modification can be explained by the decomposition of the interleaved organic DS molecules. Even if the decomposition of DS occurs at slightly higher temperatures under dynamic mode (TGA), the surfactant is found to be thermally unstable in static conditions. A basal spacing of 11 to 12 nm for the degraded hybrid phase seems to indicate the presence of interleaved sulfate anions (Sotiles and Wypych, 2019) in association with a significant loss of coherent stacking, which can be further interpreted by a process of exfoliation.

Variations in internal photoluminescence quantum yields (PL QY_{int}) as a function of the excitation wavelengths are shown for the samples treated 5 and 24 h at 120°C and for pristine LDH-DS-SRB powder in Fig. 5.

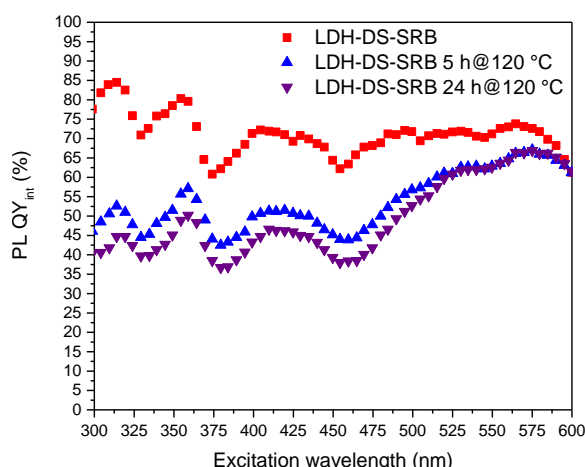


Figure 5. Variation in PL QY_{int} as a function of the excitation wavelength for LDH-DS-SRB powders, before and after thermal treatment at 120 °C.

The PL QY_{int} slightly decreases after the thermal treatment (for both exposure times) while the SRB molecule is not expected to decompose in this temperature range (Fig. 3 a). The partial loss of the stacked structure reduces the optical properties, most probably by changing the local environment of the SRB molecules. Indeed, initially stabilised by the LDH host structure as well as well dispersed and ensconced within the space supplied by the interleaved DS, the modification may cause the SRB molecules to move closer to each other. This could explain the decrease in the photoluminescence properties due to the non-radiative de-excitations.

Emission spectra of the LDH-DS-SRB powder before and after thermal treatment are compared (Fig. 6). In both cases, a wide and asymmetric emission band is observed. The maximum intensity is strongly shifted (by about 15 nm) after treatment at 120 °C. Moreover, emission intensity is found to decrease and the contribution associated with the SRB aggregates increases. At this temperature the loss of the lamellar structure, as explained before, leads to significant interactions between the SRB molecules, which are close to each other and are prone to aggregation by π -stacking (parallel stacking) due to conjugated xanthene rings or by hydrogen bonding (head-to-tail). Xanthene dyes such as SRB or fluorescein are well known to interact mutually, resulting in luminescence quenching (De and Kundu, 2011).

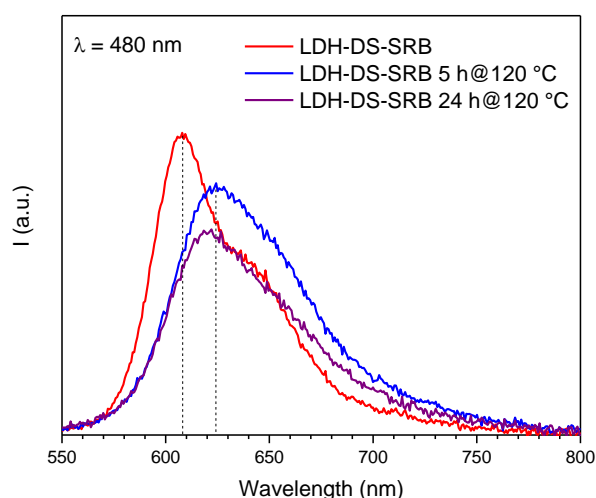


Figure 6. Emission spectra of the LDH-DS-SRB powder before and after thermal treatment at 120 °C for 5 h and 24 h ($\lambda_{exc} = 480$ nm).

The LDH-DS-SRB powders treated at 120 °C for 5 and 24 hours are shown in Fig. 7 under daylight and UV excitation (365 nm). The heat-treated powder exposed for 24 hours appears slightly darker under daylight (Fig. 7 c) than the initial powder or the sample treated for 5 hours (Fig. 7 a) and b), respectively). Under UV radiation (Fig. 7 d), e) and f), the three powders are photoluminescent with no real distinction in terms of emission intensity.

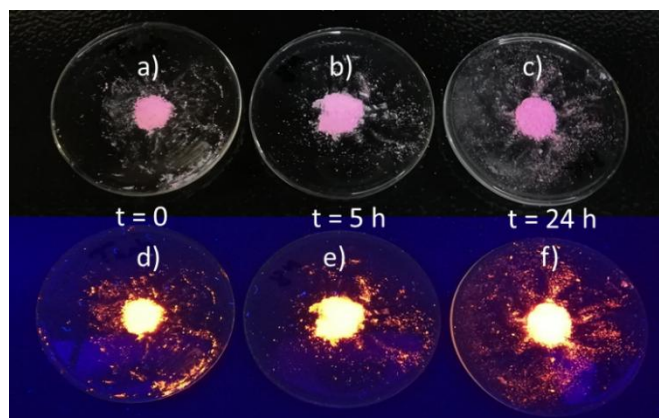


Figure 7. Initial LDH-DS-SRB powder and powders treated at 120 °C for 5 and 24 hours under daylight (a), b) and c), respectively) and under UV radiation (365 nm) (d), e) and f), respectively).

Replacing dodecylsulfate (DS) by terephthalate anions (TP)

With the aim of providing more stability, a study was performed by replacing the mono-functional surfactant DS by terephthalate anions (TP). Pioneering work showed the pillaring effect of such a di-anion form (Drezdron, 1988), which should be of interest here in stabilizing the host structure. However, the amount of interleaved TP was half the quantity of DS, while the amount of SRB was not modified. The LDH TP SRB sample was treated at 120 °C in an oven for 24 hours. The XRD patterns before and after this thermal treatment are presented in Fig. 8 a). Before thermal treatment, the powder is well crystallized, leading to a basal spacing of 1.41 nm (diffraction peak (003) at 6.3 ° in 2θ), in agreement with the literature (Drezdron, 1988). As before in the case of DS, the presence of SRB molecules cannot be detected, due to the very small amount used. After treatment, the pattern is strongly modified but the diffraction peak (003) at 6.3 ° in 2θ is still observed, meaning that the lamellar structure, even if largely degraded, is still somehow present. As expected, the 2D host structure is more robust under thermal stress thanks to a pillaring effect supplied by the TP molecules. Indeed, bi-tethered TP molecules allow an increase in the cohesion strength between layers.

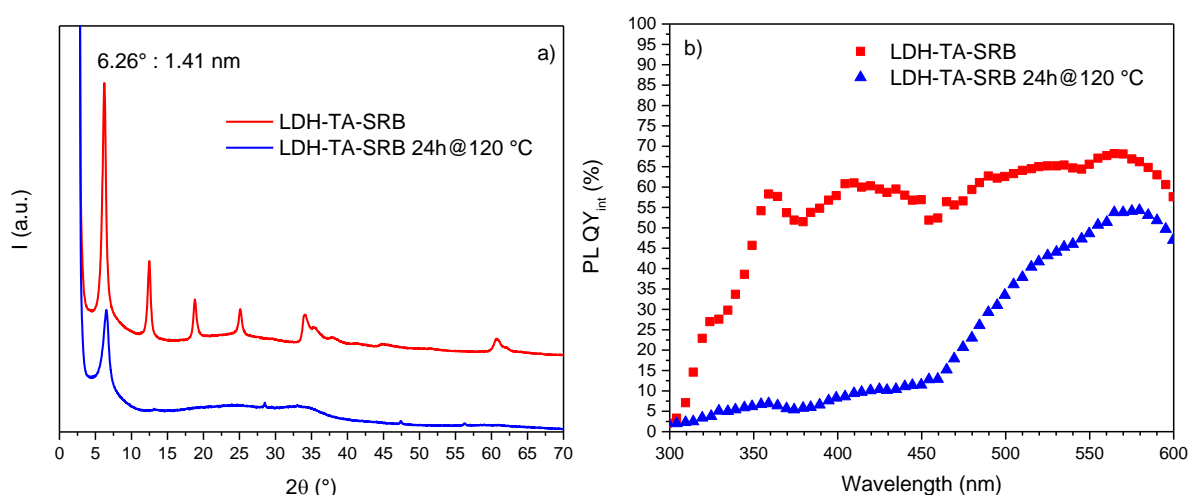


Figure 8. a) XRD patterns of LDH-TP-SRB powder and b) PL QY_{int} before and after thermal treatment at 120 °C for 24h.

PL QY_{int} was recorded before and after the thermal treatment for excitation wavelengths between 300 and 600 nm (Fig. 8 b). Before thermal treatment, the optical performances of the sample LDH-TP-SRB are generally weaker than for LDH-DS-SRB (68.1 % and 73.8 % at 570 nm respectively, for example). Moreover, photoluminescence is also thermally more affected, and the PL QY_{int} of LDH-TP-SRB decreases significantly after the treatment at 120°C; this is even more pronounced below 450 nm. At first glance, the structural cohesion supplied by TP molecules does not help to stabilize the photoluminescence properties more than in the case of the DS spacer. This is tentatively interpreted by the fact that the interlayer molecular packing is halved when replacing DS by TP, leaving the SRB molecules more space and more potential to diffuse freely, possibly causing their intermolecular interaction and thus optical quenching. For this reason, the focus is on LDH DS SRB in the following.

HTK-XRD analysis: thermal stability up to 220 °C

To unravel more precisely the structural changes occurring in the temperature domain between 25 and 220 °C, the LDH-DS-SRB powder pattern was recorded with a progressive temperature rise. The series of stacked XRD patterns recorded for each 20 °C step is shown in Fig. 9.

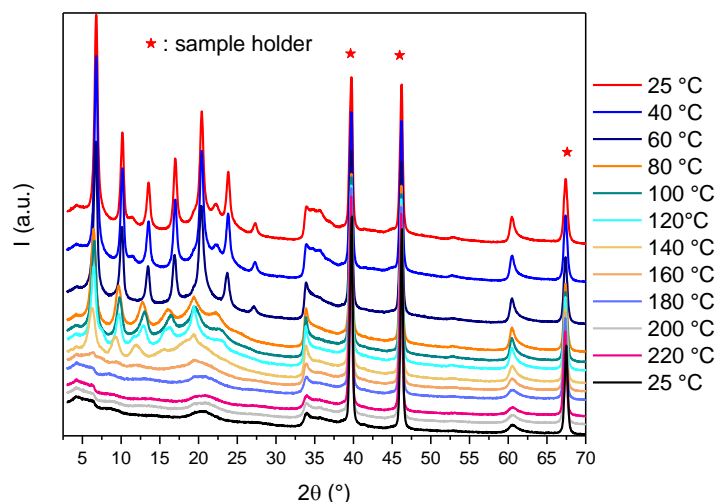


Figure 9. XRD patterns of LDH-DS-SRB powder as a function of temperature (HTK-XRD): temperature elevation of 5 °C/min followed by 15 minutes of temperature stabilisation then 1 hour of acquisition. Cooling, at 15 °C/min until reaching 25 °C, is followed by a 1-hour stabilisation period; then a final acquisition for another hour is recorded. The three intense peaks at 40°, 46° and 65° in 2θ are due to the platinum holder.

Between 25 and 60 °C, the XRD patterns are superimposed, then the intensity of the diffraction peaks (00ℓ) decreases with the temperature above 80°C, underlining that the LDH matrix is gradually losing its crystallinity in the stacking direction. Above 160°C, the diffraction peaks (00ℓ) observed below 30° in 2θ disappear, thus showing the absence of any stacking. However, the LDH sheets remain intact, with the presence of diffraction peaks at 35 and 60° in 2θ . This study confirms that the layer structure of the LDH hybrid material is lost with the decomposition of the surfactant molecules, while the LDH sheets remain after treatment at 220°C.

Photographs of LDH-DS-SRB powder under daylight and UV excitation at 365 nm before and after HTK-XRD are presented in Fig. 10. In daylight, the powder treated at 220 °C (b) is still pink, but

slightly less colourful than the initial powder (a). Under UV radiation (365 nm), photoluminescence is also still observed (d) but the emission is much weaker than initially (c). Moreover, the colour emitted by the powder excited under UV radiation is slightly different, as shown in Fig. 11. Indeed, the thermal treatment has an effect on the trichromatic coordinates, with a pronounced shift in the XY CIE diagram.

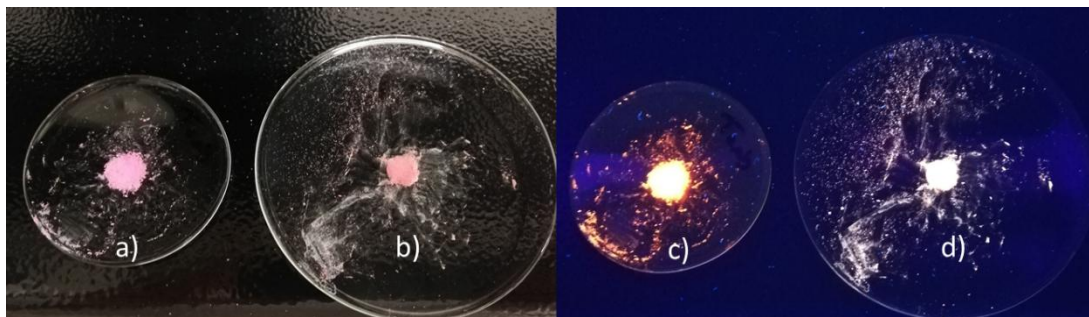


Figure 10. LDH-DS-SRB powder in daylight before (a) and after (b) HTK-XRD analysis (220 °C then cooled to 25 °C) and under UV radiation at 365 nm before (c) and after (d) this analysis.

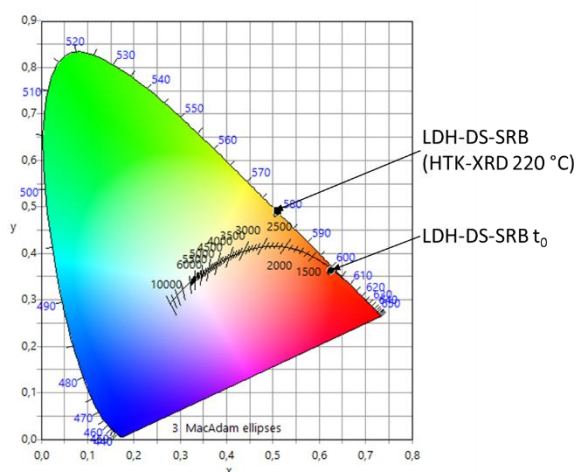


Figure 11. XY CIE 1931 diagram representing the trichromatic coordinates of the LDH-DS-SRB powder before and after HTK analysis.

The effect of the thermal treatment on the UV-vis absorption spectra of LDH-DS-SRB is shown in Fig. 12 a. The main absorption band of the SRB molecule, centred at 570 nm, is still observed after the thermal treatment at 220°C. However, the overall absorption is found after such heat treatment to increase significantly in the 400-600 nm range. This could be explained by the formation of absorbent residual product from the decomposition of the DS molecules from 120 to 150°C (Fig. 3 & 4). This is confirmed by the UV-vis absorption spectra of the LDH-DS powder (Fig. 12 b). The LDH-DS powder initially presents a white colour, whereas after heat treatment at 220°C it is black, which is consistent with the formation of carbonaceous products.

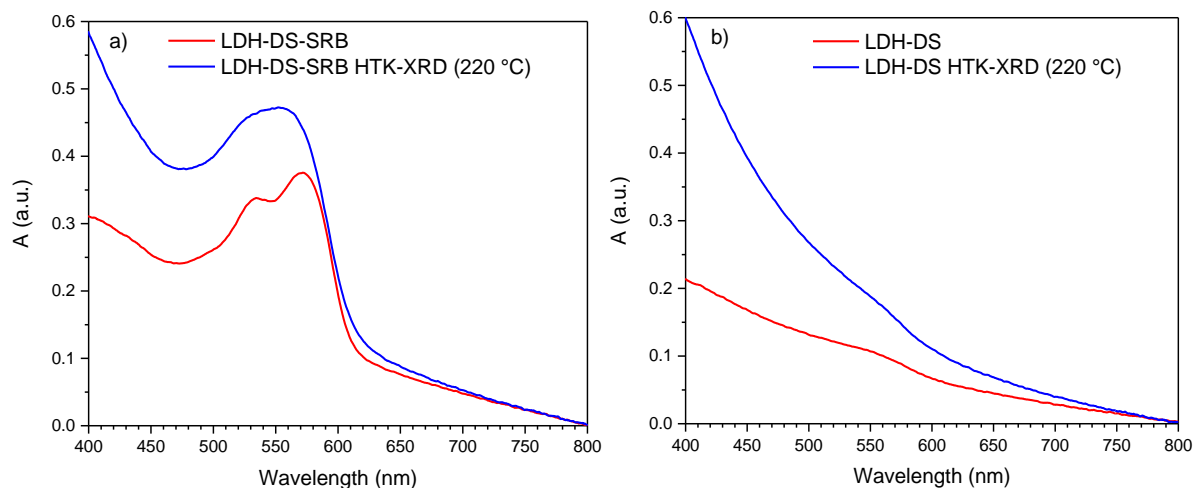


Figure 12. UV-visible spectra of a) LDH-DS-SRB and b) LDH-DS powders before and after HTK-XRD analysis.

The PL QY_{int} of the LDH-DS-SRB powders before and after thermal treatment at 220°C are reported in Table 2 for λ_{exc} = 480 and 365 nm. The drop in optical performance is clearly shown by these PL QY_{int} values.

Table 2. PL QY_{int} for λ_{exc} = 480 nm and 365 nm of LDH-DS-SRB powder before and after the HTK-XRD analysis (after cooling to 25 °C)

	Excitation wavelength	LDH-DS-SRB 25 °C	LDH-DS-SRB 220°C then cooled to 25°C
PL QY_{int} (%)	λ_{exc} = 480 nm	68.9 ± 3.5	15.0 ± 0.8
	λ_{exc} = 365 nm	73.1 ± 3.7	4.3 ± 0.2

3.2.2. Silicone/LDH-DS-SRB composite film (Si-LDS) behaviour under thermal stress

The thermal stability of the Si-LDS composite film with the optimal formulation was further studied at 120 °C for 24 h.

X-ray diffraction

XRD patterns of the Si-LDS composite film before and after the thermal treatment are presented in Fig. 13 and were compared to the pattern of the LDH-DS-SRB reference powder. First, the LDH matrix relative diffraction peaks are observed on the composite film pattern. After the thermal treatment the harmonic peaks (00 ℓ) disappear, indicating that the dispersion of the LDH-DS-SRB powder in silicone does not improve its thermal stability in terms of structural 2D integrity.

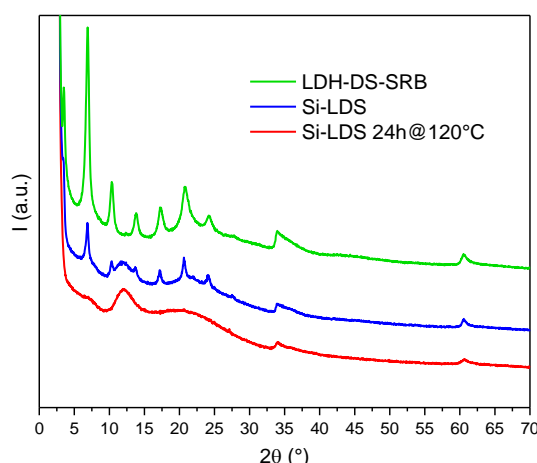


Figure 13. XRD patterns of the Si-LDS composite film before and after thermal treatment as well as the pattern of the LDH-DS-SRB powder

Optical properties

The PL QY_{int} of the composite film were recorded as a function of the excitation wavelengths before and after the thermal treatment in an oven at 120 °C for 24 hours, and are shown for each sample in Fig. 14 a. After the thermal treatment, the PL QY_{int} decreases significantly in the studied spectral range of 300-600 nm.

The emission spectrum of the composite film is shifted after the thermal treatment towards higher wavelengths (Fig. 14 b). This is the result of the aggregation of SRB molecules, as already observed with the LDH-DS-SRB reference powder (Fig. 6). The UV-Vis emission spectra also support these findings, with a significant broadening and an increase in absorption over the 550-350 nm range for the sample heat-treated at 120°C. Finally, for this thermal treatment, the PL QY_{int} of the Si-LDS composite film and of the LDH-DS-SRB powder (Fig. 5), exhibit the same change in their spectral features. However, the PL QY_{int} values recorded for the film are lower than for powder. This is in part explained by the dilution effect provided by the silicone matrix.

A film composed exclusively of silicone was also produced; it underwent the same 24-hour heat treatment at 120°C as the Si-LDS film. Recording the UV-Vis and infrared spectra led to the conclusion that the silicone does not undergo any modification after this treatment. The decrease in optical performance after the heat treatment at 120°C is thus explained, as for the powder, by an aggregation phenomenon generated by temperature.

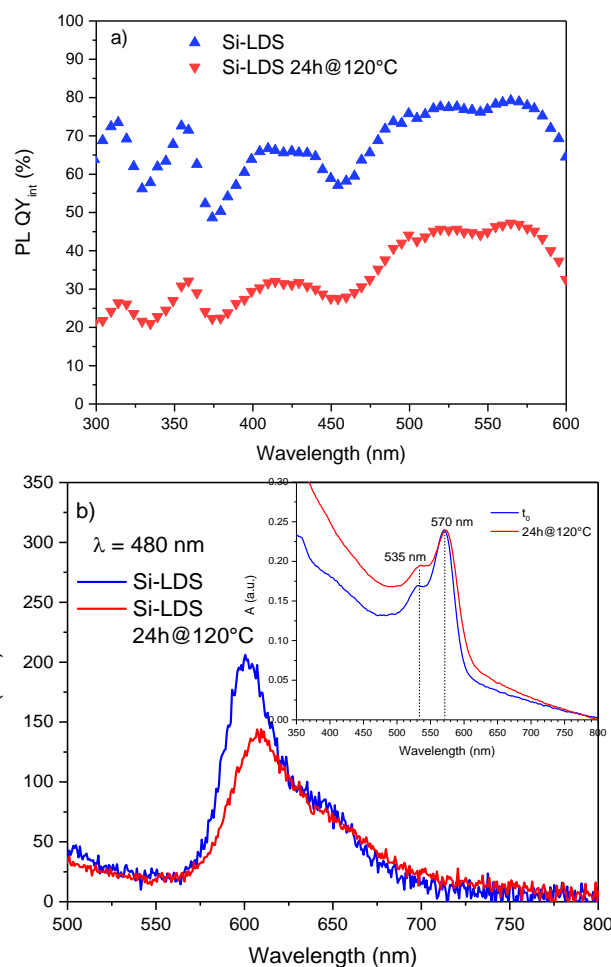


Figure 14. a) Variation in PL QY_{int} as a function of the excitation wavelength for the Si-LDS composite film before and after thermal treatment. b) Emission spectra ($\lambda_{\text{exc}} = 480 \text{ nm}$), and UV-visible spectra (inset) of the composite film before and after thermal treatment.

3.3. Composite film: durability under photonic and thermal stresses

3.3.1. Accelerated photo-aging in a SEPAP 12/24 unit

The photo-aging of the Si-LDS composite film was studied using a SEPAP 12/24 unit. In order to have a reference, a second Si-SRB composite film was produced by dispersing 0.05 %wt. pure SRB in the silicone matrix. Thus, the amounts of SRB in both films are comparable.

Fig. 15 plots PL QY_{int} as a function of irradiation time for three excitation wavelengths of interest (365, 480 and 570 nm) for Si-LDS composite film. Only the variation in the PL QY_{int} for excitation at 570 nm is provided for the S-SRB film because its luminescence is initially very low or even non-existent for excitations at 365 and 470 nm. At 570 nm, after only 3 hours, the Si-SRB film has entirely lost its luminescence, whereas the luminescence of the Si-LDS film remains identical to that observed initially, showing the benefit of the inorganic vessel for stabilizing the SRB optical properties. Quantitatively, after 35 hours the PL QY_{int} of the Si-LDS film is still above 30 %. For excitation at 365 and 480 nm, the kinetic of luminescence extinction is close to that at 570 nm.

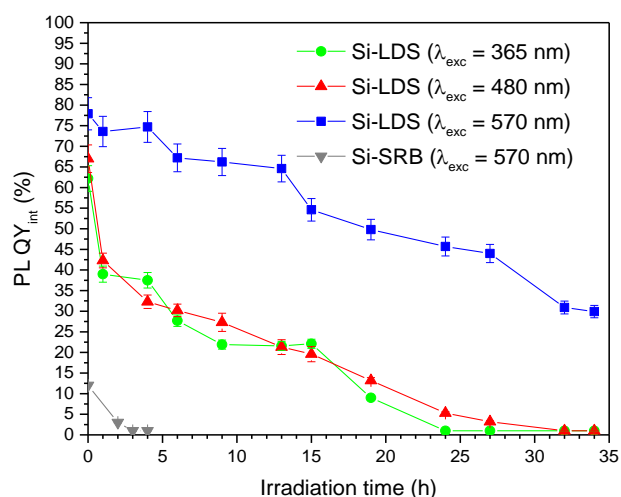


Figure 15. Variation in PL QY_{int} as a function of irradiation time in the SEPAP 12/24 unit for both Si-SRB and Si-LDS composite films for several excitation wavelengths (365, 480 and 570 nm).

In order to have a better understanding of these observations, UV-vis spectra were recorded after photo-aging. The asymmetric band relative to SRB molecules is observed for both composites before the irradiation process starts. Maximum absorbance is the same for both composites, which confirms the similar quantity of SRB molecules in both composites. However, the maximum is shifted by 20 nm between the two, and can safely be explained by a higher amount of SRB aggregates in Si-SRB than in Si-LDS.

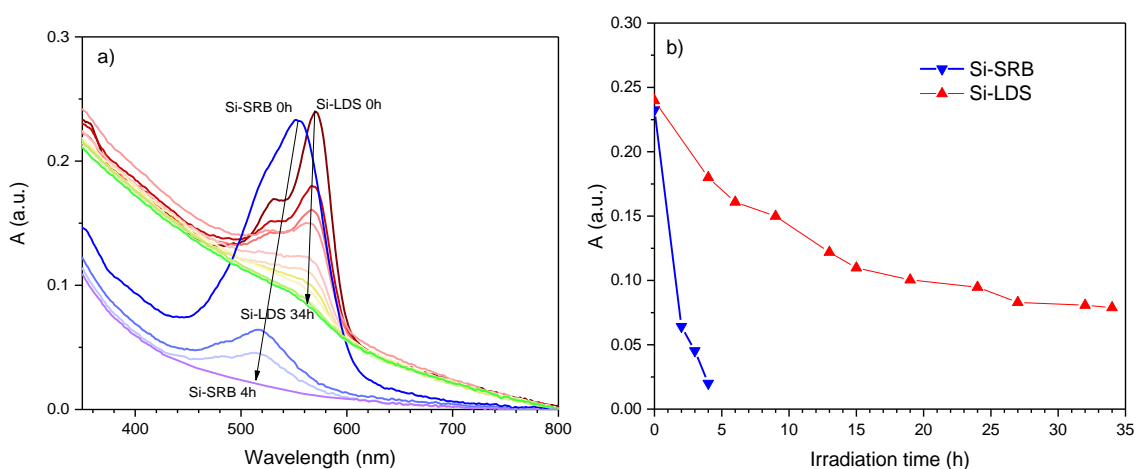


Figure 16. Variation in UV-visible spectra (a) and maximum absorbance (b) for Si-SRB and Si-LDS composites as a function of irradiation time.

During the irradiation process, the main absorbance band decreases for both composites (Fig. 16 a). The SRB molecules are irreversibly damaged by irradiation in the SEPAP 12/24 unit. However, the degradation kinetic is considerably faster for the Si-SRB film (Fig. 16 b) than for Si-LDS. Indeed, absorbance is almost extinguished after only 4 hours for the Si-SRB film, whereas a value still subsists after 34 hours for Si-LDS. This observation matches the decrease in the PL QY_{int} described above (Fig. 15).

In conclusion, the LDH host matrix makes it possible to elaborate a homogeneous composite luminescent film, but also to significantly increase SRB stability under stresses (thermal and

photonic). The conditions in the SEPAP 12/24 unit were very drastic ($\lambda > 300$ nm and $T = 60$ °C) and are not well representative of the photo-aging of composites associated with commercial blue LEDs. Nevertheless, these experiments provide information on the stability of the Si-LDS film under UV LED excitation. In the following section, the behaviour of these composites is studied in direct association with a commercial blue LED.

3.3.2. Aging under blue LED

In order to assess the stability of the Si-LDS composite film in operating conditions close to those encountered in LED devices, the Si-LDS film and the Si-SRB composite film were irradiated by a powerful blue LED (460 nm, power: 2480 W/m^2) for 1400 minutes at 80°C in a black chamber. A spectrophotometer recorded the emission spectra every 20 minutes for 24 hours.

The variation in the integrated areas of the emission spectra as a function of irradiation time is illustrated in Fig.17.

The Si-LDS composite film, using the LDH hosting the SRB molecules, is not affected at all by the stresses, and photoluminescence intensity is stable. On the contrary, the intensity of Si-SRB decreases significantly with irradiation time. A loss of 32 % was observed at the end of the first 24 hours. The beneficial effect of the LDH matrix is thus clearly demonstrated in such real conditions of use, and confirms that this Si-LDS film is fully compatible with a blue LED device.

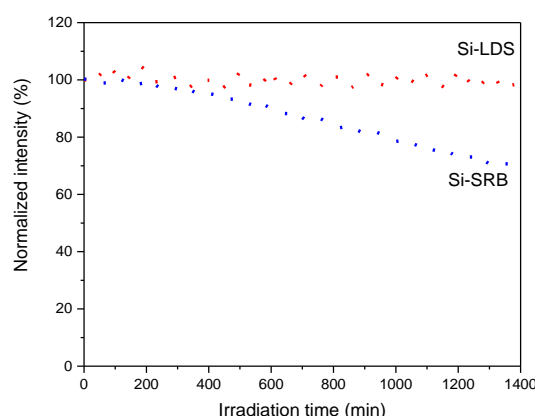


Figure 17. Variation in normalized photoluminescence intensity with respect to irradiation time for the Si-LDS and Si-SRB composite films heated to 80°C and irradiated by a commercial blue LED (460 nm, 2480 W.m^{-2}).

Photographs of both composite films, Si-SRB and Si-SDS, are presented in Fig.18 before and after the 24 h irradiation process. The colour fading of Si-SRB reveals the degradation of the SRB molecules. The aspect of Si-LDS is not modified by photo-aging; the role of LDH is well highlighted here again.

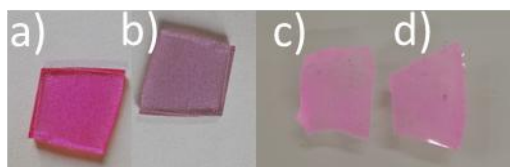


Figure 18. Photographs of Si-SRB and Si-LDS composite films before (a) and c), respectively) and after (b) and d), respectively) aging under photonic (blue LED) and thermal (80°C) stresses.

4. Conclusions

This study emphasises the ability of a LDH host structure to protect the SRB luminescent dye against various stresses. The LDH interior, filled with spacer, impedes SRB intermolecular interaction. This effect is found to be more pronounced for tightly-packed interlayer space obtained from a mono-functional co-intercalate such as DS than from TP. In the latter case, SRB molecules are freer to diffuse and thus to quench the optical properties. It is pointed out that the hybrid LDH-DS-SRB and the associated composite film exhibit a suitable orange - red emission under blue LED excitation.

The progressive loss in the optical properties of the LDH-DS-SRB hybrid powder after a treatment at 120 °C is explained by a breakdown of the LDH stacking structure, as confirmed by XRD analysis in temperature. This structural disruptive effect modifies the environment of the SRB molecules, most probably provoking their partial aggregations and thus leading to non-radiative energy transfers. Satisfactorily, a significant photoluminescence quantum yield is still observed after the thermal treatment.

Similarly, the LDH-DS-SRB/silicone composite film exhibits luminescence after thermal exposure, and this is also the case after being exposed to severe photo-aging conditions. Interestingly, the emission of the composite film when irradiated by a commercial blue LED at 80 °C to reproduce “real conditions of use” is completely stable after 24 hours. These results highlight the stability provided by the LDH host structure for dyes, and the potential of LDH-DS-SRB for commercial lighting applications based on a blue LED.

CONFLICTS OF INTEREST

There is no conflict to declare.

FORMATTING OF FUNDING SOURCES

This work was supported by CPER DEFI MMASYF through its 2016 «MetaProfile» project. Thus, the authors would like to thank the European Union in the framework of the European Regional Development Fund (ERDF), and the Région Auvergne Rhône-Alpes, which co-funded this project.

REFERENCES

- Boonsin, R., Chadeyron, G., Roblin, J.-P., Boyer, D., Mahiou, R., 2015. Development of rare-earth-free phosphors for eco-energy lighting based LEDs. *Journal of Materials Chemistry C* 3, 9580-9587.
- Conterposito, E., Benesperi, I., Toson, V., Saccone, D., Barbero, N., Palin, L., Barolo, C., Gianotti, V., Milanesio, M., 2016. High-Throughput Preparation of New Photoactive Nanocomposites. *ChemSUSchem* 9, 1279-1289.
- Cullity, B.D., 1978. *Elements of X-ray Diffraction*. Addison-Wesley Publishing Company.
- Dal Lago, M., Meneghini, M., Trivellin, N., Mura, G., Vanzì, M., Meneghesso, G., Zanoni, E., 2012. Phosphors for LED-based light sources: Thermal properties and reliability issues. *Microelectronics Reliability* 52, 2164-2167.
- Das, S., Manam, J., 2018. Fluorescein isothiocyanate and rhodamine B dye encapsulated mesoporous SiO₂ for applications of blue LED excited white LED. *Optical Materials* 79, 259-263.

De, S., Kundu, R., 2011. Spectroscopic studies with fluorescein dye—Protonation, aggregation and interaction with nanoparticles. *Journal of Photochemistry and Photobiology A: Chemistry* 223, 71-81.

Degoutin, S., Bacquet, M., Morcellet, M., 2008. Organosilica Mesoporous Materials with Double Functionality: Amino Groups and β -Cyclodextrin Synthesis and Properties, pp. 213-221.

Drezdson, M.A., 1988. Synthesis of isopolymetalate-pillared hydrotalcite via organic-anion-pillared precursors. *Inorganic Chemistry* 27, 4628-4632.

El-kharrag, R., Amin, A., Greish, Y., 2011. Synthesis and Characterization of Mesoporous Sodium Dodecyl Sulfate-Coated Magnetite Nanoparticles. *Journal of Ceramic Science and Technology* 2, 203-210.

Kajjam, A.B., Kumar, P.S.V., Subramanian, V., Vaidyanathan, S., 2018. Triphenylamine based yellowish-orange light emitting organic dyes (donor- π -acceptor) for hybrid WLEDs and OLEDs: synthesis, characterization and theoretical study. *Physical Chemistry Chemical Physics* 20, 4490-4501.

Lamouche, G., Lavallard, P., Gacoin, T., 1999. Optical properties of dye molecules as a function of the surrounding dielectric medium. *Physical Review A* 59, 4668-4674.

Legentil, P., Leroux, F., Therias, S., Boyer, D., Chadeyron, G., 2020. Sulforhodamine B-LDH composite as a rare-earth-free red-emitting phosphor for LED lighting. *Journal of Materials Chemistry C*, DOI: 10.1039/D0TC02802A

Legentil, P., Leroux, F., Therias, S., Mahiou, R., Chadeyron, G., 2019. Revisiting fluorescein and layered double hydroxide using a synergistic approach: A complete optical study. *Journal of Luminescence* 215, 116634.

Lonkar, S.P., Kutlu, B., Leuteritz, A., Heinrich, G., 2013. Nanohybrids of phenolic antioxidant intercalated into MgAl-layered double hydroxide clay. *Applied Clay Science* 71, 8-14.

Nair, G.B., Swart, H.C., Dhoble, S.J., 2020. A review on the advancements in phosphor-converted light emitting diodes (pc-LEDs): Phosphor synthesis, device fabrication and characterization. *Progress in Materials Science* 109, 100622.

Nyalosaso, J.L., Boonsin, R., Vialat, P., Boyer, D., Chadeyron, G., Mahiou, R., Leroux, F., 2019. Towards rare-earth-free white light-emitting diode devices based on the combination of dicyanomethylene and pyranine as organic dyes supported on zinc single-layered hydroxide. *Beilstein Journal of Nanotechnology* 10, 760-770.

Ogawa, M., Kuroda, K., 1995. Photofunctions of Intercalation Compounds. *Chemical Reviews* 95, 399-438.

Ray, K., Nakahara, H., 2002. Adsorption of Sulforhodamine Dyes in Cationic Langmuir–Blodgett Films: Spectroscopic and Structural Studies. *The Journal of Physical Chemistry B* 106, 92-100.

Shao, Q., Lin, H., Dong, Y., Jiang, J., 2014. Temperature-dependent photoluminescence properties of (Ba,Sr)2SiO4:Eu2+ phosphors for white LEDs applications. *Journal of Luminescence*, 165-169.

Sotiles, A.R., Wypych, F., 2019. Converting Mn/Al layered double hydroxide anion exchangers into cation exchangers by topotactic reactions using alkali metal sulfate solutions. *Chemical communications* 55, 7824-7827.

Sultana, N., 2018. Role of ammonium ion on the aggregation and adsorption properties of sodium dodecylsulfate. *Journal of Dispersion Science and Technology* 39, 92-99.

Wu, M.J., Wu, J.Z., Zhang, J., Chen, H., Zhou, J.Z., Qian, G.R., Xu, Z.P., Du, Z., Rao, Q.L., 2018. A review on fabricating heterostructures from layered double hydroxides for enhanced photocatalytic activities. *Catalysis Science & Technology* 8, 1207-1228.

Xia, Z., Xu, Z., Chen, M., Liu, Q., 2016. Recent developments in the new inorganic solid-state LED phosphors. *Dalton transactions* 45, 11214-11232.

Yan, D., Lu, J., Wei, M., G Evans, D., Duan, X., 2009. Sulforhodamine B Intercalated Layered Double Hydroxide Thin Film with Polarized Photoluminescence.

Yan, L., Wang, Y., Li, J., Kalytchuk, S., Susha, A.S., Kershaw, S.V., Yan, F., Rogach, A.L., Chen, X., 2014. Highly luminescent covalently bonded layered double hydroxide–fluorescent dye nanohybrids. *Journal of Materials Chemistry C* 2, 4490.

Yazdan Mehr, M., van Driel, W.D., Zhang, G.Q., 2014. Accelerated life time testing and optical degradation of remote phosphor plates. *Microelectronics Reliability* 54, 1544-1548.

580 Yin, Q., Li, D., Zhang, J., Zhao, Y., Wang, C., Han, J., 2019. CoNi-layered double hydroxide array on
581 graphene-based fiber as a new electrode material for microsupercapacitor. *Applied Surface Science*
582 487, 1-8.
583 Zhang, L., Li, B., Lei, B., Hong, Z., Li, W., 2008. A triphenylamine derivative as an efficient organic light
584 color-conversion material for white LEDs. *Journal of Luminescence* 128, 67-73.
585 Zhou, Z., Zhao, L., Lu, P., Zheng, H., Wang, J., Zeng, Y., 2014. Thermal influence of phosphor to GaN-
586 based white LEDs. SPIE.

587